Smoke Emission and Distribution Characteristics of Overloaded Wire Insulations under Microgravity

Hanhan Zhuang
Beihang University
Wenjun Kong (wjkong@buaa.edu.cn)
Beihang University

Research Article

Keywords: Fire safety, Microgravity, Laser extinction, Wire insulation, Overload, Smoke emission and distribution

Posted Date: April 5th, 2022

DOI: https://doi.org/10.21203/rs.3.rs-1509615/v1

Smoke Emission and Distribution Characteristics of Overloaded Wire Insulations under Microgravity

Hanhan Zhuang , Wenjun Kong*

School of Astronautics, Beihang University, Beijing, 102206, China.

*Corresponding author: Wenjun Kong, Email: wjkong@buaa.edu.cn

Abstract

With the development of manned space technology, spacecraft safety and fire prevention have attracted more and more attention. Due to the disappearance of buoyancy in microgravity, the fire early monitoring, detection and alarm technologies designed based on ground experimental results are not suitable for spacecraft. It is necessary to develop fire early monitoring technology in microgravity. Smoke is an important early monitoring signal for fire prevention both in normal gravity and microgravity. Under microgravity, fire is mostly caused by overload or aging of wire insulations. In order to study the smoke emission characteristics of wire insulations under microgravity, we carried out the overload experiments of wire insulations on board the SJ-10 Chinese recoverable satellite. The smoke generation characteristics captured by laser extinction methods, and a large number of experimental data in the real microgravity environment were obtained for the first time. In this paper, the smoke volume fractions in the early and axisymmetric stages of smoke emission from the wire insulating layer are obtained by using the method of Abel transform and convolution, and the MATLAB algorithm program is compiled. In the later stage of smoke emission, it does not show axisymmetric distribution, but the laser extinction results can be used for obtaining the smoke emission trajectory. According to the results, two smoke emission modes in the early stage of ignition of wire insulation in microgravity are quantitatively analyzed. The effects of insulation thickness, overload current and insulation material on smoke emission are discussed.

Keywords Fire safety, Microgravity, Laser extinction, Wire insulation, Overload, Smoke emission and distribution

Introduction

The growth of manned spaceflight also puts forward higher requirements for safety and stability in space. Fire safety is one of the most important problems that must be properly solved and is directly related to the safety of astronauts and the success or failure of the overall mission.

In the history of human space exploration, there have been many fire events (Thompson et al. 1967; Cortright 1970). According to NASA statistics, at least five fires occurred in the first 50 flights of the US space shuttle. Most of these accidents were caused by the abnormal behaviors of electronic and electrical components, such as wires. However, the alarm system in the spacecraft could not recognize and send out early warning signals, but abnormal smells or smoke from the fire site was detected by astronauts who subsequently found the fire (Friedman 1994). Wires are typical electrical and electronic components. Wire fault, such as aging and overload, is an important fire potential hazard in manned spaceflight.

Studies on the ignition characteristics of wire insulation in microgravity have been conducted for approximately 50 years.

Thomas et al. experimentally studied the ignition characteristics of Teflon-insulated nickel core wire with external heat source ignition on the drop tower, confirmed the characteristics of sustainable combustion of Teflon insulation in microgravity environment, and also found that the flame spread speed will be relatively reduced in microgravity

environment (Thomas et al. 1971).

Paxton et al. experimentally studied the combustion behavior of overheated wire samples for normal and microgravity conditions (Paxton et al. 1993). The wire insulation heated by the hot wire with pulse energization. The microgravity tests conducted in the 2.2 second drop tower at NASA. Three wire insulation materials representative of spacecraft application were used in the experiments, two were found to flame in microgravity but not in normal gravity. The third insulation did not flame, but there was more thermal degradation of the insulation at microgravity. Thus, the wire insulation is more likely to cause fire microgravity. The results are useful for the selection of spacecraft wire insulation (Paulos et al. 1998).

Greenberg et al. studied the flame spread characteristics of preheated polyethylene insulation in the glove box of the space shuttle (Greenberg et al. 1994; Greenberg et al.1995). The ignition of polyethylene insulation layer is realized by first energizing and preheating, and then using winding resistance wire as external ignition source from one end side. It is found that in quiescent environment, the cracking of insulating layer in microgravity environment will produce gas reaction products wrapped in wires, which is difficult to create sustainable visible flame. In the forced convection atmosphere, the phenomenon of bubble nucleation was observed in the melted insulating layer. At the same time, it was found that the flame spread rate on the surface of the insulating layer was closely related to the inlet flow direction and atmosphere.

Japanese researchers used the above similar method to carry out the wire insulation experiments on a drop tower., The wire was firstly preheated by electric current, and then ignited by an external ignition source to study the flame spread characteristics along the insulation. The used insulation material is ETFE (ethylene-tetrafluoroethylene). The sample was fixed vertically between two posts. A constant current supply was connected to the top bolt and pulley to raise the wire temperature to a given value by Joule heating of the inner wire. Then ignition was performed with a nichrome wire coil, and the downward flame spreading was observed. In the experiments, the effects of oxygen concentration, initial wire temperature, wire diameter, pressure, dilution gas and opposed external flow velocities on the combustion characteristics of the wire insulation were examined with emphasis on the flame spread rates (Kikuchi et al. 1998; Fujita et al. 2000; Fujita et al. 2002).

In addition, Parametric studies have been carried out on the effects of core on flame spread characteristics over wires for various inclination angle, ambient air flow, oxygen concentration and so on (Nakamura et al. 2009; Hu et al. 2015; Hu et al. 2017; Lv et al. 2019; Jia et al. 2022).

Huang et al. studied the ignition-to-spread transition of externally heated electrical wire (Huang et al. 2013; Huang et al. 2020). The results showed that additional heating times after flash are required in order to fully pass the transition and achieve a spreading flame. The wire core with high thermal conductivity is easy to lead to ignition failure and extinguishment of weak flame.

Korean researchers studied the effects of electric field frequency and voltage on the flame spread characteristics over wire insulations (Lim et al. 2017; Kang et al. 2021; Kang et al. 2022). The effects of the outer wire diameter, insulation thickness and core metal on flame spread over electrical wire with applying AC electric fields were experimentally investigated by varying AC frequency and voltage.

In the real case, wire overload is caused by the overheating of the core itself, which causes the insulation to ignite. Therefore, these previous studies cannot sufficiently reflect the ignition characteristics of wire overload. In particular, it is impossible to obtain the early signs of fire. Therefore, in order to develop practical flame monitoring and alarm technology of manned spacecraft, it is necessary to make a detailed and in-depth study on the early fire signs of fire caused by overload fault of wire. Therefore, we proposed the overload heating as the internal heat source to study the early temperature rise characteristics and radiation characteristics of wire under overload current. The experiment was performed on board the SJ-8 satellite (Kong et al. 2006; Kong et al. 2008; Wang et al. 2014). In the experiment, there is no external ignition source, and the wire fault is caused by its own overload heating by excessive current to simulate the

effects of a short circuit. Subsequently, other groups carried out the research on wire misfire with similar methods (Fujita et al. 2011; Shimizu et al. 2017; Fang et al. 2018).

The experimental results using this method are more in line with the practical situation of manned spacecraft. In addition to temperature variation, smoke emission is also a very important feature of the detectable signs of fire.

Previous experimental studied smoke emission characteristics by drop tower. The results showed that the smoke particles are spherical or ellipsoidal and are approximately twice as large as those produced in normal gravity, and the nature of the particle aggregates was dependent on the color of the insulation (Apostolakis et al. 1995; Srivastava et al. 1998). However, the test time of the 2.2s drop tower is too short, the smoke from the wire insulation layer doses not have enough time to generate under microgravity, and the trajectory of smoke in the confined space under microgravity cannot be obtained. Thus we suggested to investigate the smoke emission in the early stage of wire insulation by overload heating and the dispersion characteristics of the emitted smoke in the limited confined space on board SJ-10 satellite with long term microgravity (Hu et al. 2014; Hu et al. 2017; Hu et al. 2019). We have published some of these experimental results (Kong et al. 2016; Xue et al. 2019; Kong et al. 2019), two smoke emission modes, namely the end smoke jet and the bubbling smoke jet, were identified with polyethylene and polyvinyl chloride insulations.

The purpose of this paper is to process the smoke emission images from experiments completed on board SJ-10 satellite to obtain the quantitative data of the early axisymmetric stage of smoke emission from the insulation by overload heating and the trajectory distribution of subsequent smoke emission.

Microgravity Experiments on Board the SJ-10 Satellite

The microgravity experiments were carried out on board the 24th recoverable satellite of China, the SJ-10 satellite, on April 6th 2016 launched at Jiuquan Satellite Launch Center (Hu et al. 2017; Hu et al. 2019). The microgravity level is better than 10^{-3} g_0@ ≤ 0.1Hz. The wire payload was in the orbit capsule. According to the ground screening experiment, we set up 7 working conditions. To reduce the influence of motor motion noise on satellite microgravity level, we set up a sample bin. All seven wires were installed in the same sample bin. There is no need to move the samples during the experiments, and the camera can capture the images of all samples during the experiments. Figure 1 shows the sample arrangement unit in the microgravity experiment, and Table 1 shows the parameters of the seven wires. The effects of different insulation thicknesses (0.2 mm, 0.4 mm, 0.5 mm), different insulation materials (polyethylene (PE), polytetrafluoroethylene (PTFE), polyvinyl chloride (PVC)) and different overload currents (3.2 A, 3.9 A, 4.5 A) on the overload wire characteristics were studied. The core was Cr20Ni80 with a diameter of 0.5 mm, and the total resistance was 0.356 Ω. The effective length of the insulation was 40 mm and that of the core was 70 mm. The distance between the two parallel wires was 15 mm. Thermocouples were located in the middle of each wire.

Table 1 Experimental parameters of the seven wires

Test	Wire	Current, A	Material	Thickness, mm
a	#1	3.2	PE	0.20
b	#2	3.2	PE	0.40
c	#3	3.2	PE	0.50
d	#4	3.9	PE	0.40
e	#5	4.5	PE	0.40
f	#6	4.5	PTFE	0.15
g	#7	4.5	PVC	0.40

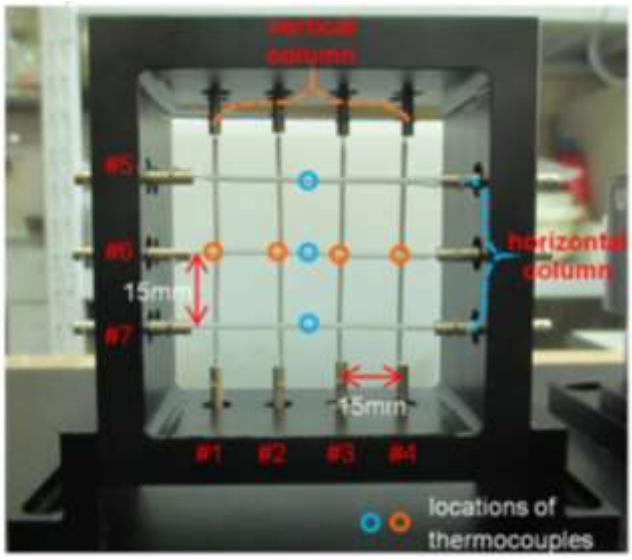

Fig. 1 Sample arrangement unit

Laser extinction method is used to measure the smoke concentration volume fraction in the early axisymmetric stage of smoke emission from the insulation by overload heating, and the subsequent laser extinction image can be used to obtain the trajectory distribution of smoke emission in the confined space. The laser light extinction measurement images were captured by CCD and a two-dimensional array of data is acquired simultaneously as used previously in microgravity (Greenberg et al. 1997). The optical path arrangement in the measurement system is shown in Figure 2. During the experiment, a beam of a stable light was emitted by the laser transmitter, which entered the convex lens after turning through the mirror. Under the action of the convex lens, the light was collimated into parallel light and entered the experimental sample unit. Then, after the beam was acted on by the beam splitter, one path directly entered CCD camera 1 to obtain the real images without extinction, and the other path entered CCD camera 2, which was equipped with a narrow-band filter to obtain images after laser extinction. During the experiment, the light source was stable, and the images were clear. An algorithm program was developed to process the image data.

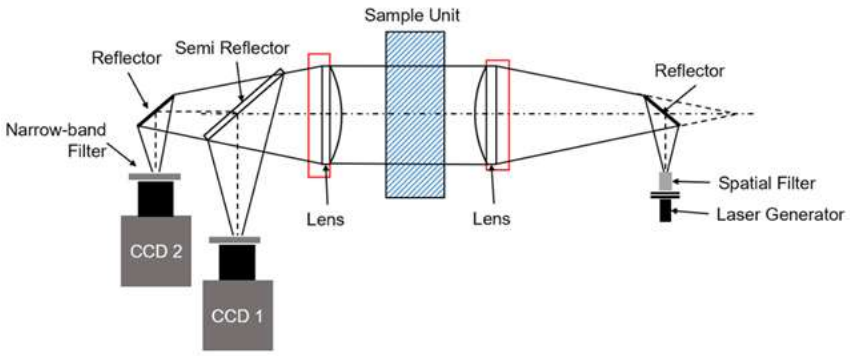

Fig. 2 Optical path arrangement in the measurement system

Data processing method

The laser extinction method is an important method to measure the volume distribution of soot in flames. Its principle is shown in Figure 3. When a laser beam passes through a flame region with soot particles, the laser intensity will be attenuated by the absorption and scattering of the soot particles. The extinction degree is related to the soot concentration. According to a certain algorithm, the soot concentration in the flame can be inverted by the images before

and after extinction, as captured by the CCD camera.

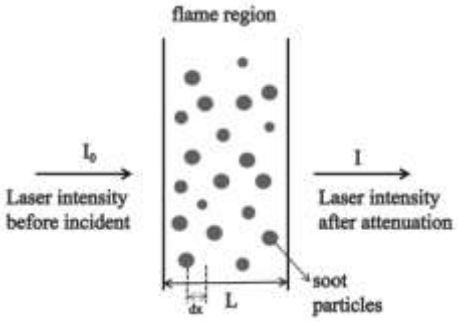

Fig. 3 Schematic diagram of laser extinction

There is a laser beam with an initial intensity I_0 and wavelength λ. According to the Lambert–Beer law, the attenuated laser intensity I can be expressed as

$$dI = -K_e I_0 dx \tag{1}$$

where dx is the optical path increment and K_e represents the extinction coefficient. The integral of Eq. (1) is

$$I = I_0 \exp\left(-\int_0^L K_e dx \right) \tag{2}$$

According to optical theory, K_e is the sum of the absorption coefficient K_a and the scattering coefficient K_s. In this study, the diameter D of the soot particles is much smaller than the laser wavelength, and the particle is approximately spherical, which meets $\frac{\pi D}{\lambda} < 0.3$. Therefore, the scattering effect of soot on the laser can be ignored (Greenberg et al. 1997; Urban et al. 1998; Konsur et al. 1999), that is, K_e is equal to K_a. According to Rayleigh's law, K_a can be given as

$$K_a = \frac{\pi^2}{\lambda} E(m) N \int_0^x P(D) D^3 \mathrm{d}D \tag{3}$$

where N is the total number of soot particles and $P(D)$ is the probability density of the size distribution of soot particles. $E(m)$ is the particle absorption term, and m is the complex absorption coefficient, which can be given by

$$E(m) = \mathrm{Im}\left| \frac{m^2 - 1}{m^2 + 2} \right| \tag{4}$$

$$m = n + ki \tag{5}$$

According to relevant research, when the wavelength is 300 nm ≤ λ ≤ 800 nm, m can be fitted with a formula with high accuracy (Iuliis et al. 1998). In this experiment, λ= 632.8 nm, and m and $E(m)$ can be calculated as follows:

$$m = 1.755 + 0.576i \tag{6}$$

$$E(m) = 0.228 \tag{7}$$

According to optical theory, the smoke concentration volume fraction f_v can be expressed as

$$f_v = \frac{\pi}{6} N \int_0^x P(D) D^3 \mathrm{d}D \tag{8}$$

By substituting Eq. (8) into Eq. (3), the relationship between f_v and K_e can finally be calculated as follows:

$$f_v = \frac{\lambda K_e}{6\pi E(m)} \tag{9}$$

Eq. (9) shows that f_v can be calculated as long as K_e is obtained. For smoke with an axisymmetric distribution, inversion algorithms can be used to calculate K_e. Dasch (1992) compared the Abel Transform algorithm, the Onion Peeling algorithm and the Filtered Projection algorithm in detail, and the Abel Transform algorithm was considered to be the best. Its calculation process was relatively easy, and the accuracy of the three-point Abel Transform was higher than that of the two-point Abel Transform. Therefore, the three-point Abel Transform algorithm is used in this study.

As shown in Figure 4, the soot concentration with an axisymmetric distribution is recorded as a function *F(r)*, and its cumulative value along the optical path x is *P(y)*. The relationship between the two is as follows:

$$P(y) = 2\int_0^{x_{\max}} F(r)dx \tag{10}$$

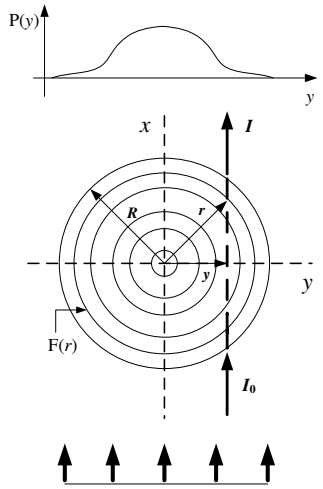

Fig. 4 Relationship between the soot distribution and the cumulative value along the path

According to Eq. (2) and Eq. (10), the following corresponding relationship can be obtained:

$$P(y) = -\ln\frac{I}{I_0} \tag{11}$$

$$F(r) = K_e \tag{12}$$

According to Eq. (12), K_e can be obtained by calculating *F(r)*.

A relationship between x, y and r can be obtained from Fig. 4. The integral variable transformation can be carried out for Eq. (10). Then, the Abel Transformation algorithm is applied, and *F(r)* can be expressed by *P(y)*:

$$F(r) = -\frac{1}{\pi}\int_r^R \frac{P'(y)}{\left(y^2 - r^2\right)^{1/2}}dy,\ y \in (r, R) \tag{13}$$

where *P(y)* represents the gray value of discrete pixels of the data in the experimental images, so Eq. (13) needs to be discretized, which can be given as

$$F(r_i) = -\frac{1}{\pi}\sum_{j=i}^{N}\int_{-\Delta r/2,\, j>i}^{0,\, j=i} \frac{P'(y_j + \delta)}{\left[(y_j + \delta)^2 - y_i^2\right]^{1/2}}d\delta \tag{14}$$

P'(y) is discretized at three points. That is, the interval (r, R) is divided into *N* cells, and the derivative value is calculated from three adjacent points (yj-Δr/2, yj, yj+Δr/2) in the interval as follows:

$$P'(y)=\left[P(y_{j+1})-P(y_{j-1})\right]/2\Delta r+\left[P(y_{j+1})+P(y_{j-1})-2P(y_j)\right]\delta/\Delta r^2 \tag{15}$$

Hence, *F(r)* can be calculated by

$$F(r_i)=\frac{1}{\Delta r}\sum_{j=0}^{N}D_{ij}P(y_j) \tag{16}$$

where D_{ij} is the operator. K_e can be calculated by Eq. (11), Eq. (12) and Eq. (16):

$$P(y_j)=-\ln\frac{I_j}{I_0} \tag{17}$$

$$K_{e,i}=F(r_i)=\frac{1}{\Delta r}\sum_{j=0}^{N}D_{ij}P(y_j) \tag{18}$$

Finally, by substituting the result into Eq. (9), the soot volume fraction and the distribution can be obtained.

In this paper, the volume concentration of smoke emission at the early axisymmetric stage can be quantitatively obtained by the above method as the soot volume fraction. The subsequent smoke emission is non-axisymmetric and can not be transformed by Abel transform. The smoke emission trajectory can be obtained by the ratio of comparing I / I_0.

Calculation of Images

The final result captured by the CCD camera is the accumulated value of smoke in the whole optical path, so signal interference along the path is inevitable. It is necessary to denoise the obtained images to obtain more accurate calculation results. According to the above, the image processing procedure can be described as follows:

(1) Image averaging. The average filtering of multiple adjacent images can solve the problem of large signal noise in a single image.

(2) Ratio images. The gray matrix of the experimental image is divided by the gray matrix of the background image to obtain the gray ratio matrix. On the one hand, fixed interference in the field of view is eliminated to a certain extent. On the other hand, the gray ratio of each pixel can reflect the absorption and scattering of the laser by solid particles in the experimental field, which is the core parameter of subsequent calculations.

(3) Gauss denoising. When the Gaussian filtering threshold is input, the noise on the image is generally expressed as a high-frequency signal. The extinction of high-frequency noise can eliminate spatial clutter and make the calculation object clearer.

(4) Boundary treatment. The boundary cutting threshold is input to address the flame boundary and its internal impurities to form a clear and meaningful boundary.

(5) Midline positioning. The gray values of two adjacent points are differentiated to find the flame boundary. The centerline is determined by using the midpoint coordinates of the left and right boundaries, and the axis position of the equivalent axisymmetric flow field is calculated.

(6) Mirror average. Taking the median line as the axis of symmetry, a rotatable surface is formed numerically to describe the axisymmetric smoke distribution.

(7) Concentration calculation. A MATLAB program was used to calculate the volume fraction of the wire smoke concentration. After judging that the data are valid, they are imported into Tecplot to generate a smoke distribution cloud map for subsequent analysis.

Results and Discussions

Quantitative Analysis of Smoke Emission Modes under Microgravity

According to the experimental results obtained from the SJ-10 payload, the temperature and smoke emission characteristics during wire overload were initial analyzed by Xue (2019). Two typical smoke emission modes in the early stage of ignition of wire insulation overload under microgravity, edge jet emission and bubble jet emission, are proposed, and the smoke emission process and morphological evolution characteristics of the two modes are described in detail. In this study, the smoke emission trajectory and concentration distribution characteristics of the two modes will be quantitatively analyzed from the calculation results of the laser extinction images.

Figure 5 shows the smoke emission trajectory and volume concentration distribution of the edge emission mode with insulation of PE, insulation thickness of 0.5 mm and current of 3.2 A . According to the principle of axisymmetry, only one side is analyzed. The dark red slender rectangular region represents the energized experimental wire, the white dotted line represents the position of adjacent wires, and the gray rectangles at both ends represent two fixed copper ports. Fig. 5 shows that smoke was emitted from both end sides of the wire, and the trajectory was symmetrically distributed at both ends. With the passage of overload time, the smoke concentration gradually increased, but the injection angle of the main jet at both ends basically did not change. In addition, due to the disappearance of natural convection in microgravity, the emitted smoke can only be transported away by diffusion, so it is very slow and the smoke could not be removed in time and accumulated at both ends of the wire. The newly generated smoke was superimposed and accumulated with the previous smoke, resulting in the formation of hemispherical smoke clouds visible to the naked eye on both sides. Due to the existence of residual buoyancy, the distribution of smoke concentration at the wire end side is uneven and asymmetric. It is seen from Fig. 5 that the volume smoke concentration the edge of the main jet was 2-10 ppm. When the smoke emission is in the edge emission mode, the accumulated smoke will jet disperse to the copper port of the adjacent wire and gather here as time went on, a high smoke concentration of 15-60 ppm will accumulated. The results in Fig. 5 also showed that the whole smoke emission process could be observed intuitively and effectively.

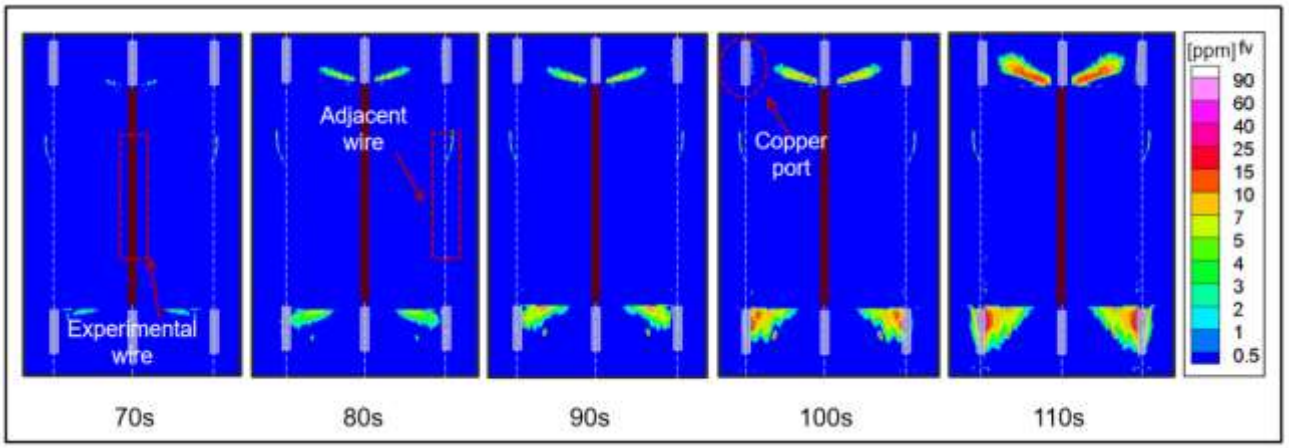

Fig. 5 Smoke emission trajectory and concentration distribution in edge injection mode (0.5 mm, PE, 3.2 A)

Figure 6 shows the smoke emission trajectory in bubbling injection mode with insulation of PVC, insulation thickness of 0.2 mm and current of 3.2 A. As time went on, the bubbling injection mode is occurrence, the smoke emission is asymmetric as show in Fig. 6. So we can obtain the trajectory distribution of smoke emission. It is seen from Fig. 6 the smoke emitted from the end side is irregular and a large amount of smoke was accumulated. While a smooth bubble appeared at the early stage of this emission mode due to pyrolysis reaction, which occurred in the insulation near the side of the core. The middle part of the insulation reached the temperature required for the reaction and began to melt,

forming a semicircular bulge. As time went on, the energy in the bubble zone reached a certain degree, and it will break and burst. A large amount of smoke will be ejected and will sweep over a large area of adjacent wires. The energy required for the anaerobic pyrolysis reaction is higher, so the overloaded core will accumulate more heat, and the temperature of the product ejected by bubbling will increase accordingly. Therefore, this mode will significantly affect the wire and other electric component near the overloaded wire, which is a space fire factor that cannot be ignored.

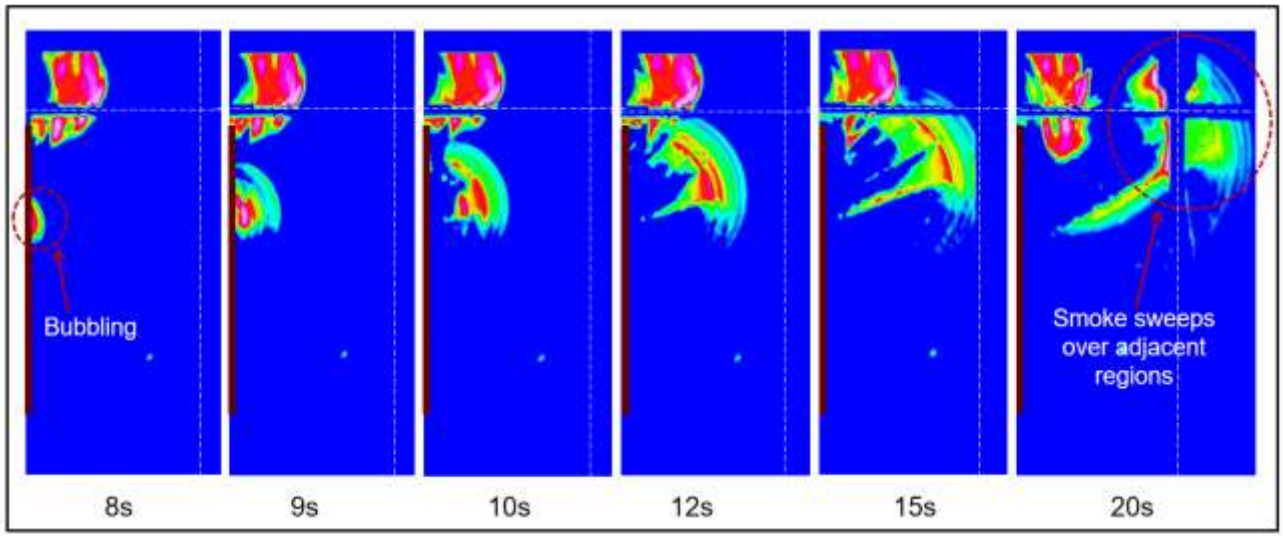

Fig. 6 Smoke emission trajectory in bubbling injection mode
(0.2 mm, PVC, 3.2 A)

Smoke Emission Characteristics under Typical Conditions

Effect of Insulation Thickness

Wires #1, #2 and #3 in Table 1 were selected to study the influence of the insulation thickness on the smoke distribution of overloaded wires. The insulation of these three wires corresponds to thicknesses of 0.2 mm, 0.4 mm and 0.5 mm respectively, and the insulation material is PE with current of 3.2 A. The calculated result is shown in Figure 7. The smoke signal was detected on the laser extinction side of wire #1 after approximately 35 s, but no obvious symmetrical edge injection mode was observed at this time. The smoke dispersion trajectory was an asymmetric bubbling jet. It appeared directly the bubbling jet mode. After 50 s later, the smoke products were distributed around the experimental wire, and the dispersion range was small. As shown in Fig. 7b, when the thickness of the insulation was 0.4 mm, smoke emission was detected on the laser extinction side after approximately 70 s. Similar to wire #1, at this time, the edge smoke emission stage had ended, and two bubbles were successively emitted and were dispersed to the adjacent wire region. After the current was continuously applied for 50 s, the bubble below also gradually increased and broke, and the emitted smoke swept over a large range of adjacent wires. When the thickness was 0.5 mm, Fig. 7c shows that the time when the smoke signal was detected was basically the same as that of wire #2. However, an obvious symmetrical edge stable injection trajectory was observed in wire #3, and this process lasted for more than 50 s. Through the above comparative analysis, the insulation thickness was found to an important factor affecting the emission time and concentration of edge smoke. With an increase in the insulation thickness, the beginning time of edge smoke emission was significantly delayed, but the duration increased. The reason for the reaction delay was that the thicker the insulation is, the more reactants there are, and the more energy needs to be accumulated before the reaction begins. However, at the same time, the more reactants there are, the more smoke products are released, and the longer the duration of smoke emission. The insulation thickness of wires #1 and #2 was so small that the concentration of smoke emitted at the edge was not enough to cause laser extinction, while the smoke emission track could clearly observed for wire #3. In addition,

the thicker the insulation is, the greater the tension that the outer surface can bear, and the later the bubbling time. More smoke products accumulated in the bubble, so the smoke dispersion range was wider.

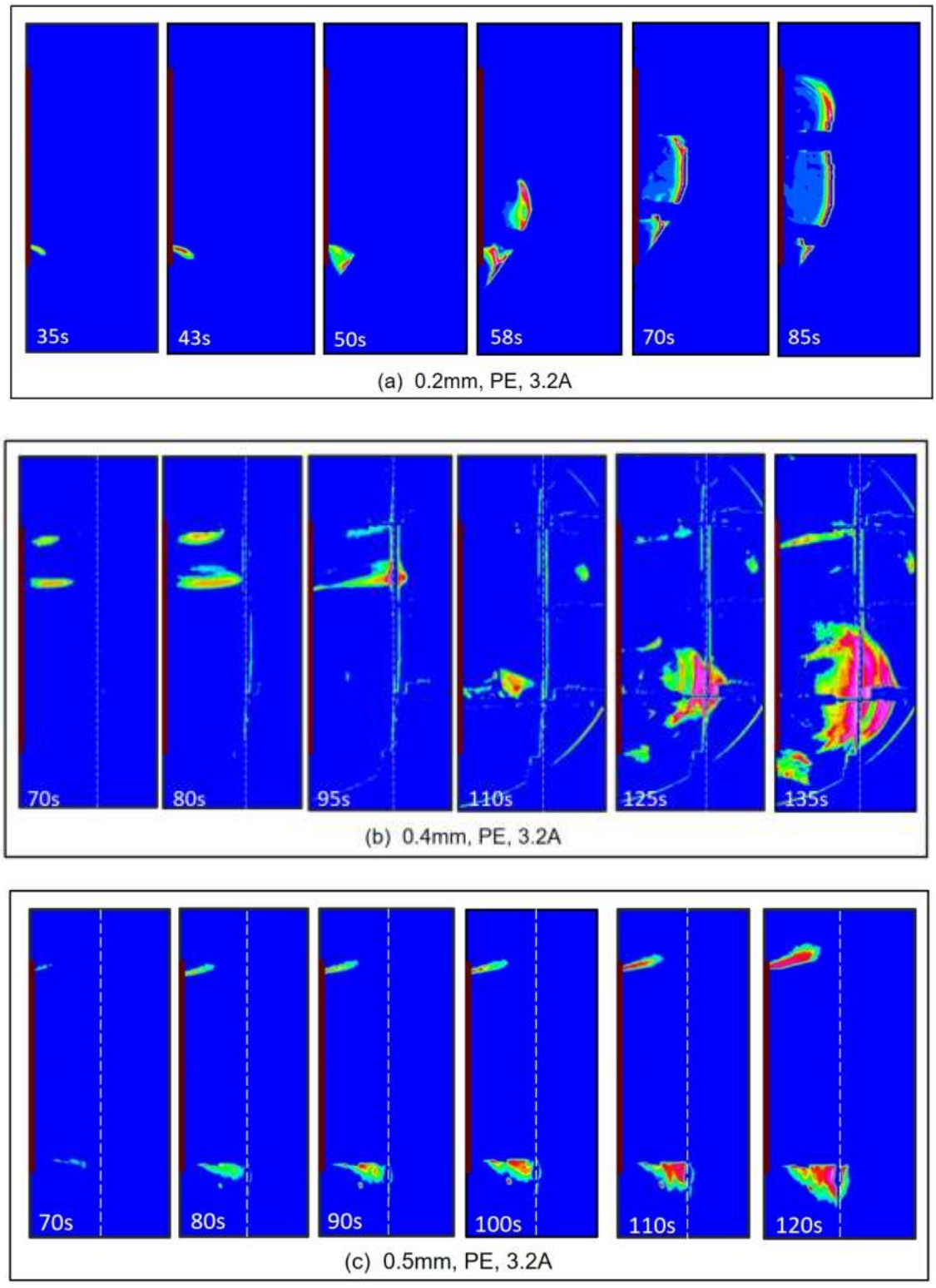

Fig. 7 Smoke emission trajectory of wires with different insulation thicknesses

Effect of Overload Current

Wire #2, #4 and #5 in Table 1 were selected to study the influence of the overload current on the smoke distribution.

The three wires correspond different currents of 3.2 A, 3.9 A and 4.5 A respectively. The insulation is PE with thickness of 0.4 mm. As shown in Figure 8, the detection times of the smoke signal under the three working conditions were 70 s, 20 s and 10 s, respectively. With the increase in current, the time needed to detect the smoke increased significantly. By comparing wires #4 and #5, it can be found that when the current was 3.9 A, the wire experienced edge jet emission mode at 20 s. When the current was 4.5 A, bubble jet emission mode began at 20 s. Therefore, the larger the current is, the shorter the evolution time of edge jet emission is, and the start time of bubble jet emission is earlier. In conclusion, the overload current is an important factor affecting the anaerobic pyrolysis rate of insulation. The increase in current will cause the time smoke emissions occur to be earlier during insulation ignition. This can be attributed to the fact that the greater the current is, the greater the power of the wire core, and the faster the pyrolysis rate of the insulation.

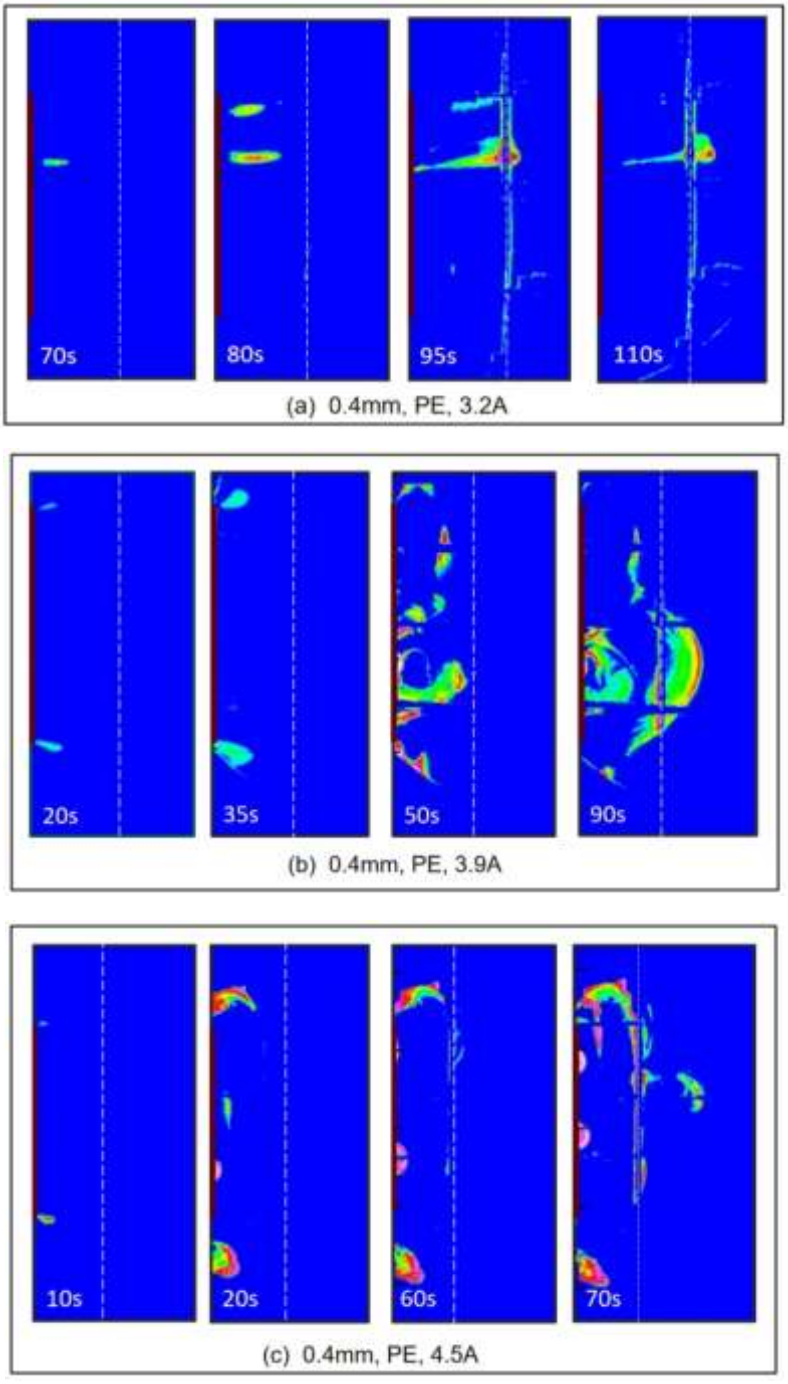

Fig. 8 Smoke emission trajectory of wires with different currents

Effect of Insulation Material

Finally, the smoke distribution when wires with different insulation materials were overloaded was analyzed. Wires #5, #6 and #7 in Table 1 corresponding respectively to PE, PTFE and PVC insulation materials were selected. The thickness of the PE and PVC insulation was 0.4 mm. The currents are 4.5 A. Due to the limitation of the experimental materials, PTFE insulation with a thickness of 0.15 mm was used in the experiment. The distribution of smoke emission trajectories of the three wires is shown in Figure 9, showing that there were great differences among the three insulation materials. As shown in Figure 9a, the smoke emission of PE insulation was mainly the evolution of two modes. The symmetrical edge jet mode was reflected in the first 15 s of overload. Then, bubbles appeared at both ends successively. The bubbles increased continuously in the evolution process, ruptured and were generated again, and the bubbles gradually moved toward the middle of the wire. The PTFE insulation mainly went through two stages when the wire was overloaded, as shown in Fig. 9b. Due to its good flame retardancy and low viscosity, unwrapping of the wrapped insulation occurred in the first stage. The second stage started at 40 s. The unwrapped insulation was wrapped around the metal wire core. After continuous heating by the current, the reaction began when the wire reaches the temperature required for pyrolysis, and a large amount of smoke was emitted and dispersed over a large space. As shown in Figure 9c, the stability of the PVC insulation was the worst when the current was overloaded. The laser extinction signal was detected at 5 s. At this time, the edge jet smoke emission mode evolved rapidly, a bubble burst and ejected products at approximately 10 s. Then, the smoke was gradually emitted along the surface of the insulation and dispersed to the adjacent wire region.

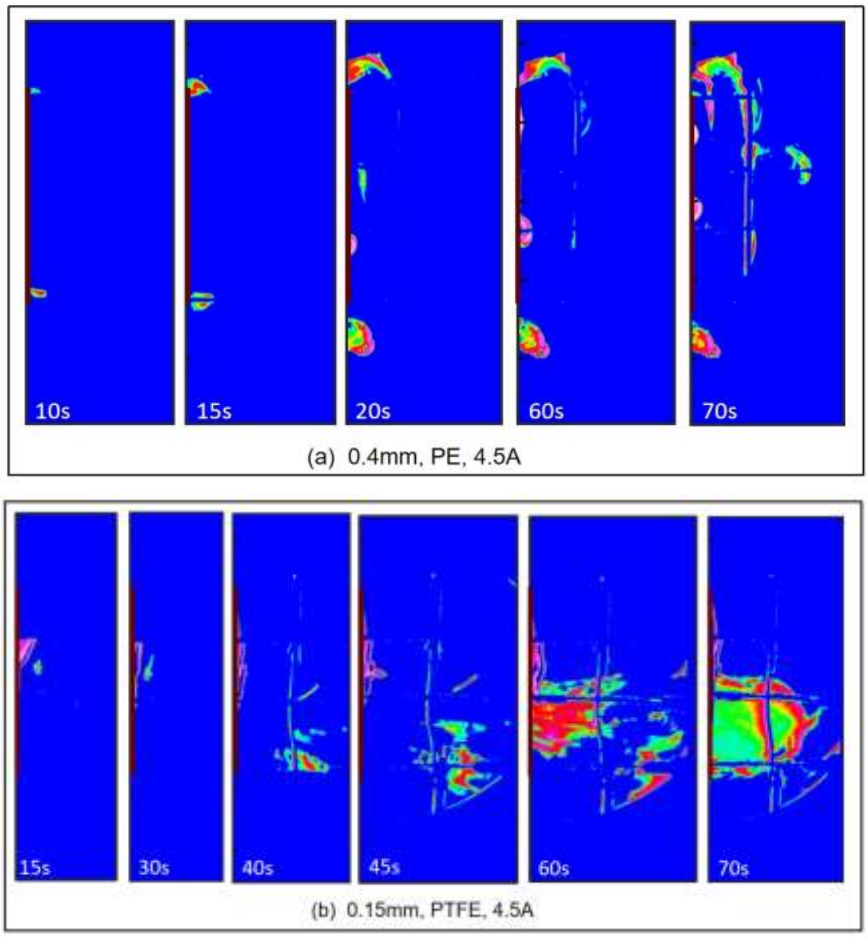

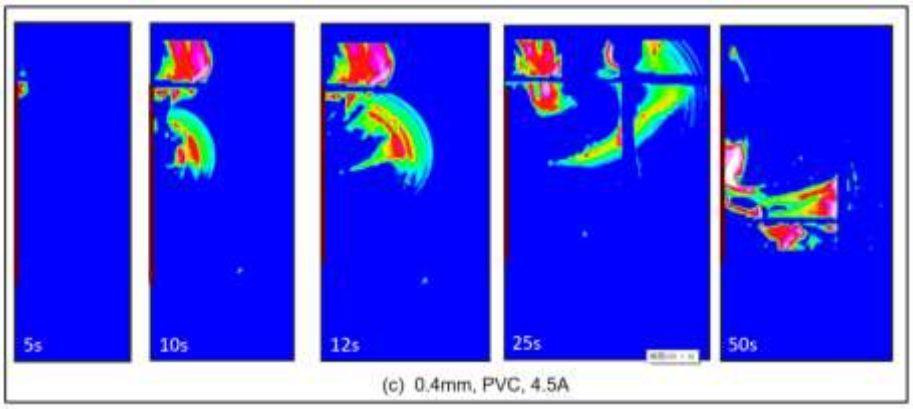

Fig. 9 Smoke emission trajectory of wires with different insulation materials

The experimental images after the experiments using the three insulation materials described above are shown in Figure 10. There was little solid residue observed after the reaction with the PE insulation, and approximately 3 mm of the insulation remained in the middle of the wire in an ellipsoid shape. After the reaction of PTFE insulation, there was no solid residue attached to the metal core, but a section of solid fragments after insulation unwinding was observed. Due to the disappearance of buoyancy in the microgravity environment, the debris was not removed in time and remained around the wire. This material is not involved in the pyrolysis reaction, so it cannot be regarded as a reaction residue. Therefore, PTFE insulation can be considered to have reacted completely. A large amount of solid residue remained in the PVC insulation after the reaction and was wrapped around the metal core in a loose cylindrical shape. This showed that there were many impurities in the PVC insulation, resulting in an incomplete reaction.

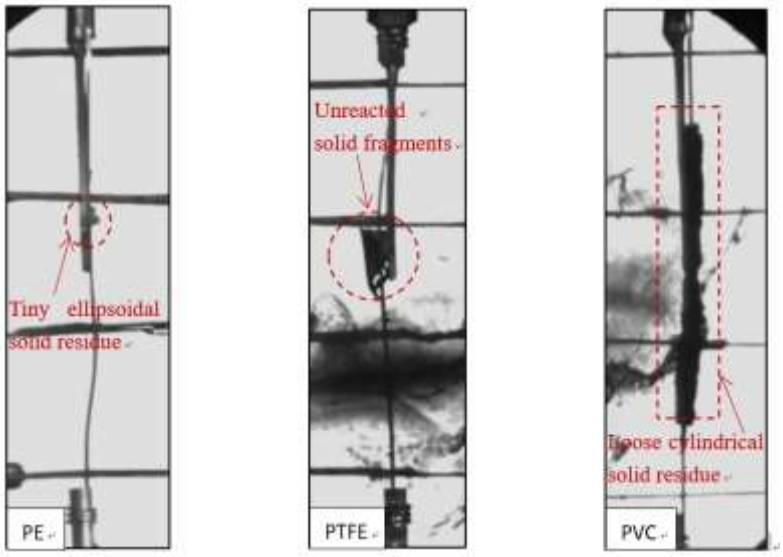

Fig. 10 Experimental images of three insulation materials after reaction

Conclusions

In this paper, the experimental data from the payload on board the SJ-10 satellite were processed and analyzed. Through the calculated results, the smoke distributions varied with time of the two smoke emission modes in the early stage of ignition of the wire insulation overload under microgravity are quantitatively obtained, and the influence characteristics of the insulation thickness, the overload current and the insulation materials on smoke distribution are obtained. The main conclusions are summarized as follows:

(1) The edge smoke emission mode plays an important role in the early ignition of wire insulation overload under

microgravity and determines the direction and concentration at the early smoke emission stage. The bubbling jet smoke emission mode will significantly affect the electronic and electrical components near the overload wires, which is a non-negligible space fire factor.

(2) The insulation thickness is an important factor affecting the emission time and concentration of smoke at the edge. With increasing thickness, the start time of the edge injection mode is delayed, and the duration of this process increases. When the start time of the bubble injection mode is delayed, the smoke products accumulated in the bubble increase, and the dispersion range of the released products is wider.

(3) The overload current is an important factor affecting the anaerobic pyrolysis rate of insulation. With an increase in the current, the power of the wire core increases, the pyrolysis rate of insulation increases, and each smoke emission time is significantly advanced.

(4) Different insulation materials produce different smoke emission trajectories when the wire is overloaded. The smoke emission of PE insulation is mainly the evolution of the edge smoke jet and bubbling smoke jet, and there is only a small amount of ellipsoid residue after the reaction; PTFE insulation has experienced two stages: unwinding and pyrolysis, and its flame-retardant performance is good. Moreover, the purity is high, the reaction is complete, and there is almost no solid residue. PVC insulation has poor flame-retardant performance and reacts violently in the initial stage of overload. The hydrocarbon bond with low activation energy breaks at the initial stage of overload and HCl gas is emitted, which can seriously endanger the safety of astronauts. There are many impurities in PVC insulation, the reaction is incomplete, and there are many solid residues. In general, PVC is not a suitable fireproof material in space.

Statements and Declarations

Funding

This work was supported by the National Natural Science Foundation of China (Grant No. U1738113). The experimental work was funded by the Strategic Priority Research Program on Space Science of the Chinese Academy of Sciences under Grant Nos. XDA04020208 and XDA04020202-08.

Conflict of Interest

The authors declare that they have no conflict of interest.

Availability of data and material

The datasets generated during and/or analyzed during the current study are available from the corresponding author on reasonable request.

Authors' contributions

Kong was the project PI. Kong and Zhuang performed the data analyses. Kong and Zhuang wrote the manuscript and Zhuang prepared figures 1-10, whereas all authors discussed the results and commented on the manuscript.

Ethics approval

Not applicable

Consent to participate

Not applicable

Consent for publication

I have read and understood the publishing policy and submit this manuscript in accordance with this policy.

References

Apostolakis, G.E., Catton, I., Issacci, F., Jones, S., Paul, M., Paulos, T., Paxton, K.: Risk-based spacecraft fire safety experiments. Reliability Eng. System Safety. 49(3), 275-291 (1995). https://doi.org/10.1016/0951-8320(95)00046-5

Cortright, E.M.: Report of APOLLO 13 review board. NASA TMX 76479, (1970)

Dasch, C.J.: One-dimensional tomography: A comparison of Abel, onion-peeling, and filtered backprojection methods. Appl. Opt. 31(8), 1146-1152 (1992). https://doi.org/10.1364/AO.31.001146

Fang, J., Zhao, S., Wang, J., Xue,Y., He,X.Z., Zhang, Y.M.: Sub-atmospheric bursting ignition of fluorinated ethylene propylene wire insulation. Fire Safety J. 100, 45-50 (2018). https://doi.org/10.1016/j.firesaf.2018.07.005

Friedman, R.: Risks and issues in fire safety on the space station. NASA TM-106430 (1994)

Fujita, O., Kikuchi, M., Ito, K.: Effective mechanisms to determine flame spread rate over Thylene-tetrafluoroethylene wire insulation: Discussion on dilution gas effect based on temperature measurements. Proc. Combust. Inst. 28(2), 2905-2911 (2000). https://doi.org/10.1016/S0082-0784(00)80715-8

Fujita, O., Nish, K., Ito, K.: Effect of low external flow on flame spread over polyethylene-insulated wire in microgravity. Proc. Combust. Inst. 29(2), 2545-2552 (2002). https://doi.org/10.1016/S1540-7489(02)80310-8

Fujita, O., Kyono, T., Kido, Y., Ito, H.,Nakamura, Y.: Ignition of wire insulation with short-term excess electric current in microgravity. Proc. Combust. Inst. 33(2), 2617-2623 (2011). https://doi.org/10.1016/j.proci.2010.06.123

Greenberg, P.S., Sacksterder, K. R., Kashiwagi, T.: Wire insulation flammability experiment: USML-1 1 year post mission summary NASA CP-3272, (1994)

Greenberg, P.S., Sacksterder, K. R., Kashiwagi, T.: Wire insulation flammability NASA CP-10174 (1995)

Greenberg, P.S., Ku, J.C.: Soot volume fraction imaging. Appl. Opt. 36(22), 5514-5522 (1997).https://doi.org/10.1364/AO.36.005514

Hu, L.H., Zhang, Y.S., Yoshioka, K., Izumo, H., Fujita, O.: Flame spread over electric wire with high thermal conductivity metal core at different inclinations. Proc. Combust. Inst. 35(3), 2607-2614 (2015). https://doi.org/10.1016/j.proci.2014.05.059

Hu, L.H., Lu, Y., Yoshioka, K., Zhang, Y.S., Fernandez-Pello, A.C., Chung, S.H., Fujita, O.: Limiting oxygen concentration for extinction of upward spreading flames over inclined thin polyethylene-insulated NiCr electrical wires with opposed-flow under normal- and microgravity. Proc. Combust. Inst. 36(2), 3045-3053 (2017). https://doi.org/10.1016/j.proci.2016.09.021

Hu, W., Zhao, J., Long, M., Zhang, X., Liu, Q., Hou, M., Kang, Q., Wang, Y., Xu, S., Kong, W., Zhang, H., Wang, S., Sun, Y., Hang, H., Huang, Y., Cai, W., Zhao, Y., Dai, J., Zheng, H., Duan, E., Wang, J.: Space program SJ-10 of microgravity research. Microgravity Sci. Technol. 26, 159–169 (2014). https://doi.org/10.1007/s12217-014-9390-0

Hu, W., Tang, B., Kang, Q.: Progress of microgravity experimental satellite SJ-10. Aeron Aero Open Access J. 1(3), 125–127 (2017). https://doi.org/10.15406/aaoaj.2017.01.00016

Hu, W.R., Kang, Q.: Physical Science under Microgravity: Experiments on Board the SJ-10 Recoverable Satellite. Beijing & Springer Nature Singapore Pte Ltd., Science Press (2019). https://doi.org/10.1007/978-981-13-1340-0

Huang, X., Nakamura, Y., Williams, F.A.: Ignition-to-spread transition of externally heated electrical wire. Proc. Combust. Inst. 34(2), 2505-2512 (2013). https://doi.org/10.1016/j.proci.2012.06.047

Huang, X., Nakamura, Y.: A Review of Fundamental Combustion Phenomena in Wire Fires. Fire Technol. 56(1), 315-360 (2020).

Iuliis, S.D., Barbini, M., Benecchi, S., Cignoli, F., Zizak, G.: Determination of the soot volume fraction in an ethylene diffusion flame by multiwavelength analysis of soot radiation. Combust. Flame. 115(1–2), 253-261 (1998). https://doi.org/10.1016/S0010-2180(97)00357-X

Jia, S., Hu, L., Ma, Y., Zhang, X., Fujita, O.: Experimental study of downward flame spread and extinction over inclined electrical wire under horizontal wind, Combust. Flame 237, 111820 (2022). https://doi.org/10.1016/j.combustflame.2021.111820

Kang, M.S. Park, S.H., Yoo, C.S., Park, J., Chung, S.K.: Effect of core metal on flame spread and extinction for horizontal electrical wire with applied AC electric fields, Proc. Combust. Inst. 38, 4747 – 4756 (2021). https://doi.org/10.1016/j.proci.2020.05.060

Kang, M.S., Park, J., Chung, S.K., Yoo, C.S.: Effect of the thickness of polyethylene insulation on flame spread over electrical wire with Cu-core under AC electric fields. Combustion and Flame, 240, 112017 (2022). https://doi.org/10.1016/j.combustflame.2022.112017

Kong, W.J., Lao, S.Q., Zhang, P.Y., Zhang, X.Q.: Study on wire insulation flammability at microgravity by functional simulation method. Combust. Sci. Technol. (in Chinese) 12(1), 1-4 (2006)

Kong, W.J., Wang, B.R., Zhang, W.K., Ai, Y.H., Lao, S.Q.: Study on prefire phenomena of wire insulation at microgravity. Microgravity Sci. Technol. 20(2), 107-113 (2008). https://doi.org/10.1007/s12217-008-9041-4

Kong, W.J., Wang, B.R., Xia, W.: Experimental facility for wire insulation combustion in SJ-10. Physics 45(4), 219-224 (2016). https://doi.org/10.7693/wl20160402

Kong, W., Wang, K., Xia, W., Xue, S.: Ignition and Combustion Characteristics of Overloaded Wire Insulations Under Weakly Buoyancy or Microgravity Environments. In: Hu W., Kang Q. (eds) Physical Science Under Microgravity: Experiments on Board the SJ-10 Recoverable Satellite. Research for Development. Springer, Singapore (2019). https://doi.org/10.1007/978-981-13-1340-0_9

Kikuchi, M., Fujita O., Ito K., Sato, A., Sakuraya, T.: Experimental study on flame spread over wire insulation in microgravity. Proc. Combust. Inst. 27, 2507-2514 (1998). https://doi.org/10.1016/S0082-0784(98)80102-1

Konsur, B., Megaridis, C.M., Griffin, D.W.: Fuel preheat effects on soot-field structure in laminar gas jet diffusion flames burning in 0-g and 1-g. Combust. Flame. 116(3), 334-347 (1999). https://doi.org/10.1016/S0010-2180(97)00297-6

Lim, S.J., Park, S.H., Park, J., Fujita, O., Keel, S.I., Chung, S.H.: Flame spread over inclined electrical wires with AC electric fields. Combustion and Flame 185, 82-92 (2017). https://doi.org/10.1016/j.combustflame.2017.07.010

Lu, Y., Huang, X., Hu, L., Fernandez-Pello, C.: The interaction between fuel inclination and horizontal wind: experimental study using thin wire, Proc. Combust. Inst. 37, 3809–3816 (2019). https://doi.org/10.1016/j.proci.2018.05.131

Paulos, T., Apostolakis, G.A.: Methodology to select a wire insulation for use in habitable spacecraft. Risk Analysis, 18(4), 471-484 (1998). https://doi.org/10.1111/j.1539-6924.1998.tb00362.x

Nakamura, Y., Yoshimura, N., Ito, H., Azumaya, K., Fujita, O.: Flame spread over electric wire in sub-atmospheric pressure. Proc. Combust. Inst. 32, 2559-2566 (2009). https://doi.org/10.1016/j.proci.2008.06.146

Paxton, K.R., Jones, S.T., Paulos, T., Issacci, F., Apostolakis, G.E., Catton, I.: Smoke and flammability of wires in microgravity. In: Proceedings of ASME Heat Transfer Division: Heat Transfer in Microgravity Systems-1993, 235, 43-48 (1993)

Shimizu, K., Kikuchi, M., Hashimoto, N., Fujita, O.: A numerical and experimental study of the ignition of insulated electric wire with long-term excess current supply under microgravity. Proc. Combust. Inst. 36(2), 3063-3071 (2017). https://doi.org/10.1016/j.proci.2016.06.134

Srivastava, R., Mckinnon, J.T., Todd, P.: Effect of Pigmentation in Particulate Formation from Fluoroploymer Thermodegradation in Microgravity. AIAA-98-0814 (1998).

Thomas, H.C., Donald, A.P.: Burning of Teflon-insulated wires in supercritical oxygen at normal and zero gravities NASA TM-2174, (1971)

Thompson, F., Borman D., Faget M.A.: Report of APOLLO 204 review board. NASA TM-84105,（1967）

Urban, D.L., Yuan, Z.G., Sunderland, P.B., Linteris, G.T., Voss. J. E.,Lin, K.C., Dai, Z., Sun, K., Faeth, G.M.: Structure and soot properties of nonbuoyant ethylene/air laminar jet diffusion flames. AIAA J. 36(8), 1346-1360 (1998). https://doi.org/10.2514/6.1998-568

Wang, K., Wang, B.R., Kong, W.J., Liu, F.S.: Study on the pre-ignition temperature variations of wire insulation under overload conditions in microgravity by the functional simulation method. J. Fire Sci. 32(3), 257-280 (2014). https://doi.org/10.1177/0734904113511947

Xue, S., Kong, W.J.: Smoke emission and temperature characteristics of the long-term overloaded wire in space. Journal of Fire Sciences 37(2), 99–116 (2019). https://doi.org/10.1177/0734904118821665